Polymer Journal (2018) 50:911–917
https://doi.org/10.1038/s41428-018-0056-4

ORIGINAL ARTICLE

Apatite coating on dendrimer-modified buckypaper and the formation of nanoapatite on MWCNTs

Tomoyuki Tajima[1] · Tomoaki Tanaka[1] · Hideaki Miyake[2] · Ill Yong Kim[3] · Chikara Ohtsuki[3] · Yutaka Takaguchi[1]

Received: 23 February 2018 / Revised: 15 March 2018 / Accepted: 16 March 2018 / Published online: 1 May 2018

Abstract

Multi-walled carbon nanotube (MWCNT)/dendrimer sheet scaffolds, i.e., dendrimers attached to the surface of MWCNT buckypaper, were fabricated, and a hydroxyapatite (HAp) coating prepared on dendrimer-modified buckypaper using an alternate soaking process (ASP) is described. The amount of the HAp that is retained on the surface of the MWCNT/dendrimer sheet scaffolds depends on the modification method; i.e., surface modification performed after the formation of the buckypaper is much more effective in producing MWCNT/HAp hybrid materials than surface modification prior to the formation of the buckypaper. Moreover, biomimetic crystallization of calcium phosphate on buckypaper in simulated body fluid (SBF) was carried out. TEM analysis of the resulting MWCNT/dendrimer sheet scaffolds revealed that the MWCNT backbone was covered with scaly crystals.

Introduction

Hydroxyapatite (HAp, $Ca_{10}(PO_4)_6(OH)_2$, HAp) has attracted great attention because of its structural and chemical similarities to the mineral components of bones [1–3], and over the past decade, particular focus has been placed on the fabrication of nanocrystalline HAp. Several studies have indicated that biomaterials containing nanocrystalline HAp exhibit a significant increase in protein adsorption and osteoblast adhesion compared to micrometer-sized Hap [4–7]. Moreover, natural bones and teeth contain HAp nanocrystals bound to the arranged type I collagen nanofibrous matrix [1, 8, 9]. During the bone formation process, a fibrous matrix of collagen is generated, followed by the precipitation of HAp minerals to form a compact bone. Therefore, fabrication of HAp-based hybrids by mimicking the biomineralization procedure has recently gained an increasing amount of attention [9–23].

On the other hand, carbon nanotubes (CNTs) are attractive in the context of material science due to not only their good mechanical, electrical, and physicochemical properties but also their similar size to triple-helical collagen fibrils, which can act as scaffolds for the induction of the nucleation and crystallization of HAp as long as they contain nucleation sites. Recently, the use of covalently [24–41] and non-covalently functionalized CNTs [42–45] as scaffolds for the growth of artificial bone material has been reported. Moreover, Bouropoulos and coworkers [25] have reported the in vitro formation of calcium phosphate on citrate-treated CNT buckypaper. These types of films represent attractive candidates for the self-repair of bone, as these sheets can persist in the body.

In this context, we have reported the synthesis of various CNT/inorganic hybrids under mild reaction conditions by biomineralization [46, 47] or sol–gel condensation reactions [48, 49]. Our method uses a water-soluble dendrimer that

Electronic supplementary material The online version of this article (https://doi.org/10.1038/s41428-018-0056-4) contains supplementary material, which is available to authorized users.

✉ Tomoyuki Tajima
tajimat@cc.okayama-u.ac.jp

✉ Yutaka Takaguchi
yutaka@cc.okayama-u.ac.jp

[1] Graduate School of Environmental Science, Okayama University, Tsushima-Naka 2-1-1, Kita-ku, Okayama 700-8530, Japan

[2] Graduate School of Sciences and Technology for Innovation, Yamaguchi University, 2-16-1 Tokiwadai, Ube, Yamaguchi 755-8611, Japan

[3] Graduate School of Engineering, Nagoya University, Furo-cho, Chikusa-ku, Nagoya 464-8603, Japan

contains affinity sites for CNTs (C_{60} or 1,10-bis(decyloxy) decane)), while poly(amidoamine) (PAMAM) dendrimers with terminal carboxylate groups function as a dispersant for the CNTs [47, 50]. These dendritic dispersants act as an effective "glue" between the CNTs and the inorganic materials, which enables the facile formation of CNT/inorganic hybrids, such as CNT/$CaCl_2$ [47], CNT/$CaCO_3$ [46, 47], CNT/SiO_2 [48], and CNT/TiO_x [49]. These results prompted us to investigate the fabrication of CNT/dendrimer sheet scaffolds and their subsequent use for the mineralization of HAp. In this paper, we report the fabrication of CNT/dendrimer sheet scaffolds, i.e., dendrimers that are attached to the surface of multi-walled carbon nanotube (MWCNT) buckypaper [51]. The subsequent mineralization of HAp on the MWCNT/dendrimer sheet scaffolds was investigated via an alternate soaking process (ASP) [52] in simulated body fluid (SBF) [53].

Experimental procedure

Instruments

Fourier transform infrared spectroscopy (FT-IR) analysis was carried out using a Shimadzu IRAffinity-1 IR spectrometer (Shimadzu, Kyoto, Japan). Scanning electron microscopy (SEM) was carried out on a Hitachi S-3500N microscope (Hitachi, Tokyo, Japan). X-ray diffraction (XRD) patterns were recorded using Cu-Kα radiation on a Rigaku RAD (Rigaku, Tokyo, Japan) at room temperature. Thermogravimetric analysis (TGA) was carried out on a Shimadzu DTG-60 in air. Quantitative energy-dispersive X-ray spectroscopy (EDX) analysis was carried out on an image obtained by a high-angle annular dark-field scanning transmission electron microscope. Transmission electron microscopy (TEM) measurements were recorded using a JEM02100 transmission electron microscope (200 kV). Water was deionized using a Millipore Milli-Q water purification system. Calcium chloride ($CaCl_2$) was purchased from Kanto Kagaku Co., Ltd. (Tokyo, Japan). Dibasic sodium phosphate (Na_2HPO_4) was purchased from Nacalai Tesque Co., Ltd. (Kyoto, Japan). MWCNTs (diameter: 20–40 nm; length: 1–2 μm; purity: 95% w/w) were purchased from Tokyo Kasei Co., Ltd. (Tokyo, Japan). Dendrimer was prepared according to previously reported procedures [47]. Buckypaper was prepared according to a previously reported method [51]. The SBF solution at pH 7.4 was prepared at 36.5 °C according to a method reported elsewhere [54].

Preparation of the MWCNT buckypaper

MWCNTs (30 mg) were suspended in *N*-methyl-2-pyrrolidone (10 mL) and sonicated for 4 h at 17–25 °C using a bath-type ultrasonic cleaner (Honda Electronics Co., Ltd., vs-D100, 110 W, 24 kHz). The resulting suspension was filtered through a membrane filter with a pore size of 0.45 μm (diameter: 2.5 cm, Merck Millipore Ltd.) using an all-glass filtration apparatus [55]. The prepared film was stored for 2 days in a vacuum desiccator containing freshly activated silica gel. The film (29.7 mg, diameter: 2 cm) was gently handled and carefully peeled off the surface of the membrane filter.

Preparation of MWCNT/dendrimer sheet scaffolds that contain 9 wt% dendrimer (MWCNT-D9wt% sheet)

The protocol for the formation of MWCNT-D9wt% sheets is as follows: pristine buckypaper (5 mg, 5 mm × 5 mm) cuttings were soaked for 13 h at room temperature in an aqueous solution (2 mL) of dendrimer (5 mg, 2.74 μmol). After storing the MWCNT/dendrimer sheet scaffolds for 2 days in a vacuum desiccator containing P_2O_5, MWCNT-D9wt% sheets (5.8 mg) were obtained. The content of dendrimer in the MWCNT/dendrimer sheet scaffold was estimated based on TGA measurements.

Preparation of MWCNT-D14wt% sheets

MWCNTs (30 mg) were suspended in an aqueous solution (10 mL) of dendrimer (30 mg, 16.5 μmol) and sonicated for 4 h at 17–25 °C using a bath-type ultrasonic cleaner (Honda Electronics Co., Ltd., vs-D100, 110 W, 24 kHz). The resulting suspension was filtered through a membrane filter (pore size: 0.45 μm; diameter: 2.5 cm; Merck Millipore Ltd.) using an all-glass filtration apparatus [55]. The sheet obtained in this manner was stored for 2 days in a vacuum desiccator containing P_2O_5 before the sheet (25.3 mg) was carefully peeled off from the surface of the membrane filter. The content of dendrimer in the MWCNT/dendrimer sheet scaffolds was estimated based on TGA measurements (14 wt%).

Fabrication of MWCNT/HAp (ASP)

An ASP was performed to promote the formation of HAp on the surface of the buckypaper. Initially, the MWCNT/dendrimer sheet scaffold (5 mg; 5 mm × 5 mm) was soaked in an aqueous solution of $CaCl_2$ (10 mL, 0.2 M, pH = 7–8) at 38 °C. After 30 min, the sheet was washed with acetone and dried. Then, the MWCNT/dendrimer sheet scaffold was soaked for 30 min in an aqueous solution of Na_2HPO_4 (10 mL, 0.12 M, pH = 8–9) at 38 °C. After washing with small portions of water and acetone, the film was dried. These steps represent one cycle. The ASP was repeated for a variable number of cycles, as outlined in the individual experiments.

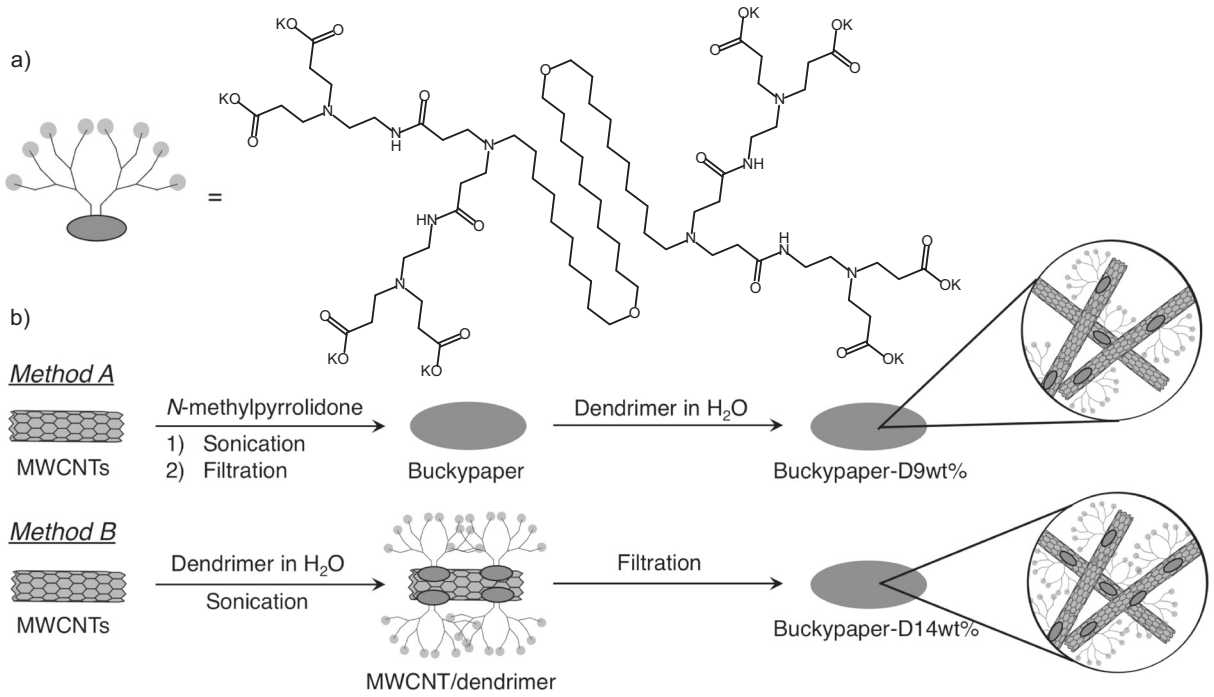

Fig. 1 **a** Schematic illustration of the dendrimer used in this study. **b** Fabrication of MWCNT/dendrimer sheets

The content of HAp was estimated based on the weight of the residue at 700 °C from TGA measurements.

Fabrication of MWCNT/HAp (SBF process)

The MWCNT/dendrimer sheet scaffold (MWCNT-D9wt%, 5.0 mg, 5 mm × 5 mm) was immersed in SBF (prepared with pH = 7.4 at 36.5 °C) and kept at 60 °C for 14 days. After washing with small portions of water and acetone, the resulting film was stored in a vacuum desiccator containing P_2O_5 to afford the MWCNT/HAp hybrid (6.3 mg).

Results and discussion

PAMAM dendrimers with a 1,10-bis(decyloxy)decane core [48] (Fig. 1a) were used as a glue to form MWCNT/HAp hybrids. MWCNT/dendrimer sheets were prepared by two different methods. In method A, MWCNT buckypaper, which was fabricated by vacuum filtration of MWCNTs dispersed in *N*-methylpyrrolidone, was soaked in an aqueous solution of dendrimer (Fig. 1b, method A). The dendrimer contents in the MWCNT/dendrimer sheets obtained in this manner (9 wt%; MWCNT-D9wt%) were determined by TGA in air (Figure S1). In method B, MWCNT/dendrimer sheets were directly fabricated by vacuum filtration of an aqueous solution of the MWCNT/dendrimer composite (Fig. 1b, method B), which afforded MWCNT/dendrimer sheets containing 14 wt% dendrimer (MWCNT-D14wt%).

HAp was mineralized on the MWCNT-D9wt% sheets using an ASP, which is a well-established and facile method for the formation of HAp on materials [52, 56]. For that purpose, MWCNT-D9wt% sheets were alternately soaked in solutions that contain either calcium or phosphate ions, whereby one cycle lasts 60 min, i.e., 30 min in the calcium-containing solution and 30 min in the phosphate-containing solution, to fabricate the MWCNT/HAp hybrids. Figure 2 shows SEM images of the MWCNT-D9wt%/HAp hybrids that were obtained by subjecting MWCNT-D9wt% sheets to 1, 2, 3, or 5 soaking cycles. After 1 or 2 soaking cycles, the obtained sheets retained the fibrous morphology of the MWCNTs. Interestingly, small spheres attached to the MWCNT-D9wt% sheet surface were clearly observable, and the number of spheres increased with the number of soaking cycles. These results suggest that HAp mineralizes on the MWCNT-D9wt% sheets. Figure S2 shows XRD patterns of the fabricated MWCNT/HAp hybrids. The main diffraction peak at 26.08° can be attributed to the graphite plane (002) of the MWCNTs. The peaks at 31.64° (211) and 39.28° (310) are a close match with the diffraction from HAp (JCPD card number: 34-0010). These peaks sharpen and increase in intensity with increasing number of soaking cycles, which suggests that the amount of crystalline HAp increases with the number of soaking cycles. To characterize the as-prepared nanohybrids, their chemical

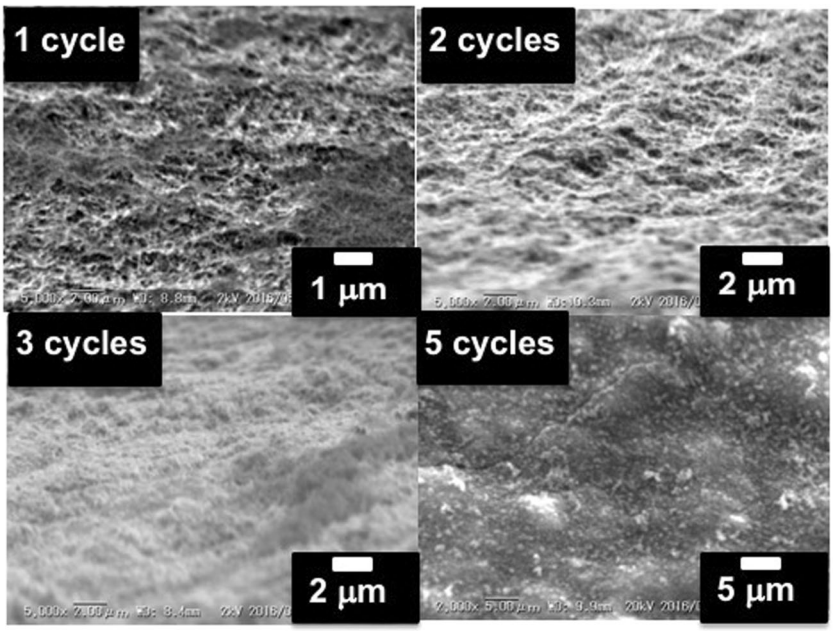

Fig. 2 SEM images of the MWCNT-D9wt%/HAp hybrids obtained by exposing MWCNT-D9wt% to 1, 2, 3, or 5 soaking cycles

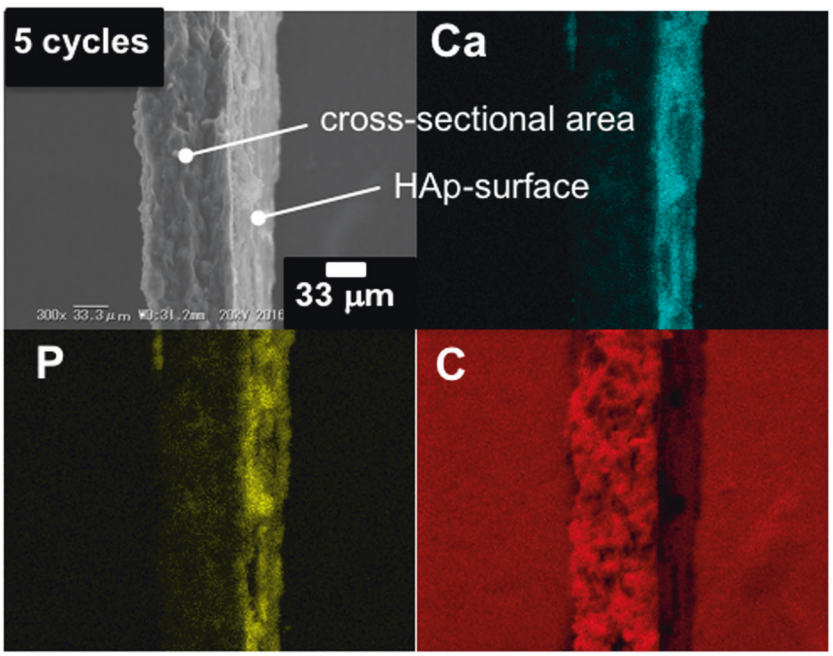

Fig. 3 Cross-sectional SEM images of a MWCNT-D9wt %/HAp hybrid obtained from 5 soaking cycles. Mapping of Ca, P, and C in the sample cross-section

composition was analyzed by EDX, and the corresponding EDX spectra are shown in Figure S3. The pronounced Ca and P signals on the buckypaper surface suggest the formation of HAp. The Ca/P ratio determined by EDX reached 1.62 after 5 soaking cycles, which is in good agreement with the value for $Ca_{10}(PO_4)_6(OH)_2$ (HAp). Figure 3a shows a cross-sectional SEM image of the MWCNT/HAp hybrids. The mapping of the elements on the sample cross-section revealed homogeneous deposition of Ca (Fig. 3b), P (Fig. 3c), and C (Fig. 3d) on the surface of the MWCNT-D9wt% sheet. The chemical structure of HAp on the MWCNT-D9wt% sheet was examined by FT-IR. Characteristic peaks at approximately 1034 and 590 cm^{-1} (Figure S4) are assignable to the P–O stretching of the phosphate groups [57]. These results strongly support the formation of HAp on the surface of the MWCNT-D9wt% sheets.

To investigate the influence of the dendrimer content, we also investigated the mineralization of HAp on MWCNT-D14wt% and pristine buckypaper (MWCNT-D0wt%).

Small spheres similar to those attached to the surface of the MWCNT-D9wt% sheets were also observed in the SEM images of the MWCNT-D14wt%/HAp hybrids (Figure S5). However, it seems that the amount of Hap on the MWCNT-D14wt%/HAp hybrids is lower than that on the MWCNT-D9wt%/HAp hybrids. Figure S6 depicts TGA thermographs of the MWCNT-D0wt%/HAp, MWCNT-D9wt%/HAp, and MWCNT-D14wt%/HAp hybrids, wherein weight loss in the range of 300–450 °C is considered to signify decomposition of the dendrimer. A more substantial weight loss caused by the decomposition of the MWCNTs was observed in the range of 500–600 °C (600–700 °C for MWCNT-D0wt%/HAp). The weight of the residue from each run at 700 °C was assigned exclusively to HAp. For the MWCNT-D0wt%/HAp, MWCNT-D9wt%/HAp, and MWCNT-D14wt%/HAp hybrids, HAp contents of 0.7, 12.5, and 5.5 wt%, respectively, were estimated. This result indicates that dendrimers provide nucleation sites and effectively act as a glue between the CNTs and HAp, even though the amount of Hap decreases with increasing dendrimer content. This trend is most likely due to differences associated with the nucleation sites on the surface of the MWCNTs. Higher amounts of dendrimers may cause higher binding levels of calcium ions, corresponding to a depletion of these ions in solution, which could inhibit nucleation.

To probe potentially beneficial aspects and the utility of the physical modifications of buckypaper with dendrimers, we carried out biomimetic crystallization of calcium phosphate on a MWCNT/dendrimer sheet in SBF. For this purpose, MWCNT-D9wt% sheets were immersed into SBF and kept at 60 °C for 14 days under static conditions in order to crystallize HAp. TEM analysis of the resulting buckypaper film revealed that the MWCNT backbone was covered in scaly crystals (Fig. 4). In the case of the pristine buckypaper (MWCNT-D0wt%), only very few particles were observed on the MWCNTs (Figure S7), although EDX analysis revealed significant adsorption of calcium and phosphate ions from the SBF (Ca:P = 1.40). Even though this ratio is smaller than the ideal ratio of HAp (1.67), the result indicates that the Ca^{2+} and PO_4^{3-} ions at least interact with the surface of the buckypaper with the help of the dendrimer scaffold. Another important biomaterial in this context is β-tricalcium phosphate (TCP), which shows in vivo resorbability during bone tissue ingrowth [58]. In addition, the interaction between β-TCP and body fluids results in HAp formation after implantation [59]. Therefore, we investigated the sintering of the MWCNT/apatite hybrid (Ca:P = 1.40) obtained from SBF to potentially fabricate MWCNT/TCP sheets. After sintering of the MWCNT/apatite hybrid (Ca:P = 1.40) at 1000 °C, MWCNT/β-TCP sheets were obtained. The XRD pattern of the sintered MWCNT/apatite hybrid (Ca:P = 1.40) is shown in Figure S8. The sharp peaks of the recorded XRD pattern are consistent with the characteristics of β-TCP according to the Joint Committee on Powder Diffraction Standards card (JCPDS) PDF No. 9–169.

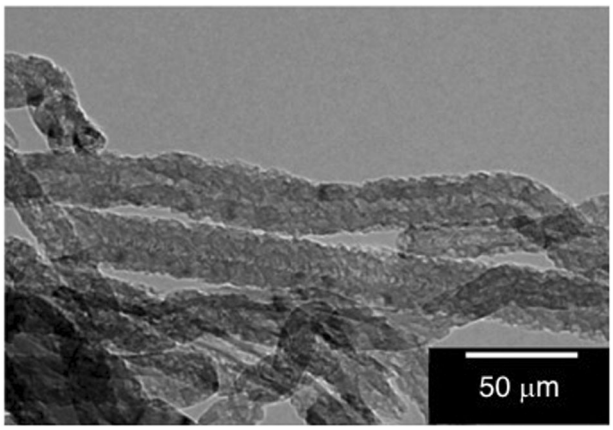

Fig. 4 TEM image of a dendrimer-modified buckypaper (MWCNT-D9wt%) after immersion for 14 days in SBF at 60 °C

Conclusions

The crystallization of HAp on buckypaper, whose surface was modified with PAMAM dendrimers that contain a 1,10-bis(decyloxy)decane core, using an ASP was investigated. Moreover, the biomimetic crystallization of HAp on dendrimer-modified buckypaper from SBF was investigated. SEM and TEM analyses of the MWCNT/HAp hybrids revealed that HAp successfully mineralizes on the surface of these MWCNTs. These CNT/dendrimer sheets should become useful for the production of synthetic HAp as a bone replacement and for the investigation at the nano-bio interface on the growth of nerve cells.

Acknowledgements This work was partially supported by a Grant-in-Aid for Scientific Research (No. 25107723; Y.T. and No. 22107007; C.O.) on Innovative Areas of "Fusion Materials" (No. 2206) and JSPS KAKENHI grants 15H03519 (Y.T.) and 16K05895 (T.T.). The authors would like to express their sincerest gratitude to the Division of Instrumental Analysis, Department of Instrumental Analysis & Cryogenics, Advanced Science Research Center, Okayama University, for the XRD, SEM, and EDX measurements.

Compliance with ethical standards

Conflict of interest TThe authors declare no conflict of interest.

References

1. Dorozhkin SV, Epple M. Biological and medical significance of calcium phosphates. Angew Chem Int Ed. 2002;41:3130–46.
2. Wopenka B, Pasteris JD. A mineralogical perspective on the apatite in bone. Mater Sci Eng C. 2005;25:131–43.

3. Lakes R. Materials with structural hierarchy. Nature. 1993;361:511–5.
4. Webster TJ, Ergun C, Doremus RH, Siegel RW, Bizios R. Specific proteins mediate enhanced osteoblast adhesion on nanophase ceramics. J Biomed Mater Res. 2000;51:475–83.
5. Webster TJ, Siegel RW, Bizios R. Osteoblast adhesion on nanophase ceramics. Biomater. 1999;20:1221–7.
6. Wei G, Ma PX. Structure and properties of nano-hydroxyapatite/polymer composite scaffolds for bone tissue engineering. Biomater. 2004;25:4749–57.
7. Sadat-Shojai M, Khorasani M-T, Dinpanah-Khoshdargi E, Jamshidi A. Synthesis methods for nanosized hydroxyapatite with diverse structures. Acta Biomater. 2013;9:7591–621.
8. Tathe A, Ghodke M, Nikalje AO. A brief review: biomaterials and their application. Int J Pharm Pharm Sci. 2010;2:19–23.
9. Kim S, Park CB. Bio-inspired synthesis of minerals for energy, environment, and medicinal applications. Adv Funct Mater. 2013;23:10–25.
10. Xu A-W, Ma Y, Cölfen H. Biomimetic mineralization. J Mater Chem. 2007;17:415–49.
11. Nishimura T, Imai H, Oaki Y, Sakamoto T, Kato T. Preparation of thin-film hydroxyapatite/polymer hybrids. Chem Lett. 2011;40:458–60.
12. Tanahashi M, Yao T, Kokubo T, Minoda M, Miyamato T, Nakamura T, Yamamuro T. Apatite coating on organic polymers by a biomimetic process. J Am Ceram Soc. 1994;77:2805–8.
13. Collins AM, Skaer NJV, Gheysens T, Knight D, Bertran C, Roach HI, Oreffo ROC, Von-Aulock S, Baris T, Skinner J, Mann S. Bone-like resorbable silk-based scaffolds for load-bearing osteoregenerative applications. Adv Mater. 2009;21:75–8.
14. Nudelman F, Pieterse K, George A, Bomans PHH, Friedrich H, Brylka LJ, Hilbers PAJ, With G. Sommerdijk NAJM, the role of collagen in bone apatite formation in the presence of hydroxyapatite nucleation inhibitor. Nat Mater. 2010;9:1004–9.
15. Dey AD, Bomans PHH, Müller FA, Will J, Frederik PM, With G, Sommerdijk NAJM. The role of prenucleation clusters in surface-induced calcium phosphate crystallization. Nat Mater. 2010;9:1010–4.
16. Imai H, Tatara S, Furuichi K, Oaki Y. Formation of calcium phosphate having a hierarchically laminated architecture through periodic precipitation in organic gel. Chem Commun. 2003;39:1952–3.
17. Yokogawa Y, Nagata F, Toriyama M, Nishizawa K, Kameyama T. Inhibition of calcium phosphate formation on polymeric substrate in the presence of polyacrylic acid. J Mater Sci Lett. 1999;18:367–8.
18. Girija EK, Yokogawa Y, Nagata F. Apatite formation on collagen fibrils in the presence of polyacrylic acid. J Mater Sci Mater Med. 2004;15:593–9.
19. Miyazaki T, Ohtsuki C, Akioka Y, Tanihara M, Nakao J, Sakaguchi Y, Konagaya S. Apatite deposition on polyamide films containing carboxyl group in a biomimetic solution. J Mater Sci Mater Med. 2003;14:269–74.
20. Kawai T, Ohtsuki C, Kamitakahara M, Miyazaki T, Tanihara M, Sakaguchi Y, Konagaya S. Coating of an apatite layer on polyamide films containing sulfonic groups by a biomimetic process. Biomater. 2004;25:4529–34.
21. Sugawara A, Yamane S, Akiyoshi K. Nonogel-templated mineralization: Polymer-calcium phosphate hybrid nanomaterials. Macromol Papid Commun. 2006;27:441–6.
22. Antonietti M, Breulmann M, Göltner CG, Cölfen H, Wong KK, Walsh WD, Mann S. Inorganic/organic mesostructures with complex architectures: precipitation of calcium phosphate in the presence of double-hydrophilic block copolymers. Chem Eur J. 1998;4:2493–500.
23. Song J, Malathong V, Bertozzi CR. Mineralization of synthetic polymer scaffolds: a bottom-up approach for the development of artificial bone. J Am Chem Soc. 2005;127:3366–72.
24. Akasaka T, Watari F, Sato Y, Tohji K. Apatite formation on carbon nanotubes. Mater Sci Eng C. 2006;26:675–8.
25. Tasis D, Kastanis D, Galiotis C, Bouropoulos N. Growth of calcium phosphate mineral on carbon nanotube buckypapers. Phys Stat Sol B. 2006;243:3230–3.
26. Lei T, Wang L, Ouyang C, Li NF, Zhou LS. In situ preparation and enhanced mechanical properties of carbon nanotube/hydroxyapatite composites. Int J Appl Ceram Technol. 2011;8:532–9.
27. Khalid P, Hussain MA, Rekha PD, Arun AB. Synthesis and characterization of carbon nanotubes reinforced hydroxyapatite composite. Indian J Sci Technol. 2013;6:5546–51.
28. Mukherjee S, Kundu B, Chanda A, Sen S. Effect of functionalization of CNT in the preparation of HAp–CNT biocomposites. Ceram Int. 2015;41:3766–74.
29. Rajesh R, Senthilkumar N, Hariharasubramanian A, Ravichandran YD. Review on hydroxyapatite-carbon nanotube composites and some of their applications. Int J Pharm Sci. 2012;4:23–7.
30. Lee M, Ku SH, Ryu J, Park CB. Mussel-inspired functionalization of carbon nanotubes for hydroxyapatite mineralization. J Mater Chem. 2010;20:8848–53.
31. Marsi TCO, Santos TG, Pacheco-Soares C, Corat EJ, Marciano FR, Lobo AO. Biomineralization of superhydrophilic vertically aligned carbon nanotubes. Langmuir. 2012;28:4413–24.
32. Zanin H, Rosa CMR, Eliaz N, May PW, Marciano FR, Lobo AO. Assisted deposition of nano-hydroxyapatite onto exfoliated carbon nanotube oxide scaffolds. Nanoscale. 2015;7:10218–32.
33. White AA, Best SM. Hydroxyapatite-carbon nanotube composites for biomedical applications: a review. Int J Appl Ceram Technol. 2007;4:1–13.
34. Lee H-H, Shin US, Won J-E, Kim H-W. Preparation of hydroxyapatite-carbon nanotube composite nanopowders. Mater Lett. 2011;65:208–11.
35. White AA, Kinloch JA, Windle AH, Best SM. Optimization of the sintering atmosphere for high-density hydroxyapatite-carbon nanotube composites. J R Soc Interface. 2010;7:S529–39.
36. Bai Y, Neupane MP, Park IS, Lee MH, Bae TS, Watari F, Uo M. Electrophoretic deposition of carbon nanotubes-hydroxyapatite nanocomposites on titanium substrate. Mater Sci Eng C. 2010;30:1043–9.
37. Wahab R, Ansari SG, Kim YS, Mohanty TR, Hwang IH, Shin HS. Immobilization of DNA on nano-hydroxyapatite and their interaction with carbon nanotubes. Synth Met. 2009;159:238–45.
38. Mei F, Zhong J, Yang X, Ouyang X, Zhang S, Hu X, Ma Q, Lu J, Ryu S, Deng X. Improved biological characteristic of poly(L-lactic acid) electrospun membrane by incorporation of multiwalled carbon nanotubes/hydroxyapatite nanoparticles. Biomacromolecules. 2007;8:3729–35.
39. Zhao HY, Zhou HM, Zheng W, Zheng YF. Carbon nanotube-hydroxyapatite nanocomposite: A novel platform for glucose/O_2 biofuel cell. Biosens Bioelectron. 2009;25:463–8.
40. Zhao HY, Xu XX, Zhang JX, Zheng W, Zheng YF. Carbon nanotube-Hydroxyapatite-hemoglobin nanocomposites with high bioelectrocatalytic activity. Bioelectrochemistry. 2010;78:124–9.
41. Mukherjee S, Mohammadi H, Azimi M, Hafezi M, Osman NAA. Synthesis and characterization of β-TCP/CNT nanocomposite: Morphology, microstructure and *in vitro* bioactivity. Ceram Int. 2017;43:7573–80.
42. Singh MK, Shokuhfar T, Joaquim J, Gracio A, Carlos A, Sousa CM, Fereira JMDF, Garmestani H, Ahzi S. Hydroxyapatite modified with carbon-nanotube-reinforced poly(methyl methacrylate): a nanocomposite material for biomedical applications. Adv Func Mater. 2008;18:694–700.

43. Li A, Sun K, Dong W, Zhao D. Mechanical properties, microstructure and histocompatibility of MWCNT/HAp biocomposites. Mater Lett. 2007;61:1839–44.
44. Li X, Lan J, Ai M, Guo Y, Cai Q, Yang X. Biomineralization on polymer-coated multi-walled carbon nanotubes with different surface functional groups. Colloids Surf B Biointerfaces. 2014;123:753–61.
45. Venkatesan J, Qian Z-J, Ryu B, Mumar NA, Kim S-K. Preparation and characterization of carbon nanotube-grafted-chitosan – natural hydroxyapatite composite for bone tissue engineering. Carbohydr Polym. 2011;83:569–77.
46. Tajima T, Tsutsui A, Fujii T, Takada J, Takaguchi Y. Fabrication of novel core-shell microspheres consisting of single-walled carbon nanotubes and $CaCO_3$ through biomimetic mineralization. Polym J. 2012;44:620–4.
47. Nishimura S, Tajima T, Hasegawa T, Takaguchi Y, Oaki Y, Imai H. Synthesis of poly(amidoamine) dendrimer having a 1,10-bis (decyloxy)decane core and its use in fabrication of carbon nanotube/calcium carbonate hybrids through biomimetic mineralization. Can J Chem. 2017;95:935–41.
48. Tajima T, Sakata W, Wada T, Tsutsui A, Nishimoto S, Miyake M, Takaguchi Y. Photosensitized hydrogen evolution from water using a single-walled carbon nanotube/fullerodendron/SiO_2 coaxial nanohybrid. Avd Mater. 2011;23:5750–4.
49. Kurniawan K, Tajima T, Kubo Y, Miyake H, Kurashige W, Negishi Y, Takaguchi Y. Incorporating a TiO_x shell in single-walled carbon nanotube/fullerodendron coaxial nanowires: Increasing the photocatalytic evolution of H_2 from water under irradiation with visible light. RSC Adv. 2017;7:31767–70.
50. Takaguchi Y, Tamura M, Sako Y, Yanagimoto Y, Tsuboi S, Uchida T, Shimamura K, Kimura S, Wakahara T, Maeda Y, Akasaka T. Fullerodendron-assisted dispersion of single-walled carbon nanotubes via noncovalent functionalization. Chem Lett. 2005;34:1608–9.
51. Oh JY, Yang SJ, Park JY, Kim T, Lee K, Kim YS, Han HN, Park CR. Easy preparation of self-assembled high-density buckypaper with enhanced mechanical properties. Nano Lett. 2015;15:190–7.
52. Taguchi T, Kishida A, Akashi M. Hydroxyapatite formation on/in poly(vinyl alcohol) hydrogel using a novel alternate soaking process. Chem Lett. 1998;27:711–2.
53. Kokubo T, Kushitani H, Sakka S, Kitsugi T, Yamamoto T. Solutions able to reproduce *in vivo* surface-structure changes in bioactive glass-ceramic A-W^3. J Biomed Mater Res. 1990;24:721–34.
54. Cho SB, Nakanishi K, Kokubo T, Soga N, Ohtsuki C, Nakamura T, Kitsugi T, Yamamuro T. Dependence of apatite formation on silica gel on its structure: effect of heat treatment. J Am Ceram Soc. 1995;78:1769–74.
55. Hussein L, Urban G, Krüger M. Fabrication and characterization of buckypaper-based nanostructured electrodes as a novel material for biofuel cell applications. Phys Chem Chem Phys. 2011;13:5831–9.
56. Sun X, Uyama H. In situ mineralization of hydroxyapatite on poly (vinyl alcohol) monolithic scaffolds for tissue engineering. Colloid Polym Sci. 2014;292:1073–8.
57. Matsusaki M, Kadowaki K, Tateishi K, Higuchi C, Ando W, Hart DA, Tanaka Y, Take Y, Akashi M, Yoshikawa H, Nakamura N. Scaffold-free tissue-engineered construct-hydroxyapatite composites generated by an alternate soaking process: Potential for repair of bone defects. Tissue Eng Part A. 2009;15:55–63.
58. Bohner M. Silicon-substituted calcium phosphates – a critical view. Biomater. 2009;30:6403–6.
59. Wang W, Zhu Y, Liao S, Li J. Carbon nanotubes reinforced composites for biomedical applications. BioMed Res Int. 2014;2014:518609. 1–14